RESEARCH ARTICLE | NOVEMBER 11 2014

High quality boron carbon nitride/ZnO-nanorods p-n heterojunctions based on magnetron sputtered boron carbon nitride films

J. C. Qian; S. K. Jha; B. Q. Wang; E. V. Jelenković; I. Bello; J. E. Klemberg-Sapieha; L. Martinu; W. J. Zhang

Appl. Phys. Lett. 105, 192104 (2014)
https://doi.org/10.1063/1.4901273

High quality boron carbon nitride/ZnO-nanorods p-n heterojunctions based on magnetron sputtered boron carbon nitride films

J. C. Qian,[1,2] S. K. Jha,[3,a)] B. Q. Wang,[4] E. V. Jelenković,[5] I. Bello,[6]
J. E. Klemberg-Sapieha,[2] L. Martinu,[2] and W. J. Zhang[1,a)]
[1]*Department of Physics and Materials Science and Center of Super-Diamond and Advanced Films, City University of Hong Kong, HKSAR, China*
[2]*Department of Engineering Physics, Polytechnique Montréal, Montreal, Quebec H3A 3A7, Canada*
[3]*Blackett Laboratory, Department of Physics, Imperial College London, London SW7 2AZ, United Kingdom*
[4]*Department of Mechanical and Materials Engineering and Department of Chemistry, University of Western Ontario, London, Ontario N6A 5B8, Canada*
[5]*State Key Laboratory in Ultra-Precision Machining Technology, Department of Industrial and Systems Engineering, The Hong Kong Polytechnic University, HKSAR, China*
[6]*Vacuum Electronics Ltd., London, Ontario N6K 5A2, Canada*

(Received 1 September 2014; accepted 28 October 2014; published online 11 November 2014)

Boron carbon nitride (BCN) films were synthesized on Si (100) and fused silica substrates by radio-frequency magnetron sputtering from a B_4C target in an Ar/N_2 gas mixture. The BCN films were amorphous, and they exhibited an optical band gap of ~1.0 eV and p-type conductivity. The BCN films were over-coated with ZnO nanorod arrays using hydrothermal synthesis to form BCN/ZnO-nanorods p-n heterojunctions, exhibiting a rectification ratio of 1500 at bias voltages of ±5 V.
 [http://dx.doi.org/10.1063/1.4901273]

Boron carbon nitride (BCN) is an attractive material due to its structural similarity to carbon (graphite and diamond) and boron nitride (BN in hexagonal and cubic phases). The hexagonal BCN (*h*-BCN) has tunable electrical characteristics that fall between semi-metallic graphite and insulating hexagonal BN (*h*-BN),[1] while the cubic BCN (*c*-BCN) shows properties comparable to diamond and cubic BN (*c*-BN).[2] BCN films have been synthesized by a variety of techniques including chemical vapor deposition (CVD)[3–5] and physical vapor deposition (PVD).[6,7] In contrast to the C and BN phase segregation commonly observed in *c*-BCN films,[8,9] the synthesis of the ternary *h*-BCN phase is available as confirmed by X-ray absorption near-edge spectroscopy (XANES).[10] Preliminary studies suggest that *h*-BCN is a p-type semiconductor with a band gap strongly dependent on the elemental composition.[11–13] Interestingly, amorphous BCN films were synthesized at lower substrate temperatures while their tunable electrical properties could still be maintained.[14] The low deposition temperature reduces the manufacturing cost and makes it possible to carry out the deposition on substrates with low melting points, such as flexible plastics.[15] Thus far, there have been only very few studies on the electronic devices based on BCN to a large extent due to the complex phase structure varying with the deposition parameters and the film composition.

Very interesting device applications of BCN have been predicted, and several related patents have been granted.[16] In particular, boron-containing materials are well known as good candidates for applications in solid state neutron detection because of the high neutron capture cross section of boron.[17] Various p-n junction neutron detectors based on semiconducting boron carbide (BC) have been fabricated, such as homojunctions made by doping,[18] heterojunctions formed with other materials,[19,20] and "heteroisomeric" junctions composed of undoped p- and n-type BC.[21] Combining the high neutron capture ability and unique semiconducting properties, BCN can potentially be the material of choice for fabricating neutron detection devices. Therefore, p-n junctions based on BCN are very important to investigate for practical applications.

ZnO, as an inherent n-type semiconductor,[22] is a very attractive material to form p-n heterojunctions with p-type BCN. As inspiration, ZnO nanorods (NRs) have been used as building blocks in active electronic and optoelectronic devices, such as transistors, light emitting diodes,[23,24] and solar cells.[25,26] In response, in this work, we present a heterojunction diode made of BCN/ZnO-NRs using simple growth of ZnO NRs on BCN films. We show a representative I-V characteristic of the BCN/ZnO-NRs heterojunctions and demonstrate a rectification ratio of 1500.

BCN films were prepared by RF (13.56 MHz) magnetron sputtering from a single B_4C target (75 mm in diameter). The films, with a thickness of ~1 μm, were deposited on Si (100) and fused silica substrates. Prior to deposition, the system was pumped down to a base pressure of $<1.0 \times 10^{-4}$ Pa, and the sputtering process was carried out using a gas mixture of N_2:Ar with a flow rate ratio of 2:8 and a total flow rate of 10 sccm at a pressure of 0.4 Pa. An RF power of 200 W was applied to the B_4C target, and the substrate holder was electrically grounded. The substrates were not intentionally heated, and the substrate temperature reached about 90 °C due to plasma heating.

In the subsequent step, arrays of vertical ZnO NRs were grown over the BCN film using a low-temperature (95 °C) hydrothermal growth process.[27,28] Thus, both the BCN and ZnO materials were processed at temperatures below 100 °C and hence required little thermal budget.

a)Authors to whom correspondence should be addressed. Electronic addresses: skylec@gmail.com and apwjzh@cityu.edu.hk.

The structure of the BCN films was studied by Fourier transform infrared spectroscopy (FTIR) (FT-IR 1600, Perkin-Elmer). The elemental composition and the chemical structure of the films deposited on silicon were analyzed by X-ray photoelectron spectroscopy (XPS) using a VG ESCALAB 220i-XL ultrahigh vacuum (UHV) surface analytical facility with a base pressure of 10^{-7} Pa. A monochromatic Al Kα (1486.6 eV) X-ray source was used, and the XPS spectra were taken after Ar ion sputter cleaning of the sample surface. A Lambda-750 UV/Vis spectrophotometer was used to record absorption spectra and analyze optical properties of the BCN films on fused silica. The Hall measurements were carried out at 5000 G and room temperature using a Lakeshore 7704A system. The morphology of the ZnO NRs was studied by scanning electron microscopy (SEM, Philips FEG SEM XL30). The electrical characterization of the BCN/ZnO-NRs heterojunction diodes was performed using a Keithley-4200 semiconductor parameter analyzer.

A representative FTIR spectrum of the as-deposited BCN films is presented in Fig. 1. Two distinct absorption bands can be observed. The narrow band located at 780 cm^{-1} is assigned to the out-of-plane B−N−B bending vibration, whereas the broad band centered around 1400 cm^{-1} can be attributed to the in-plane B−N stretching vibration.[29] However, this broad band extended over a wide wavenumber range from 1000 to 1800 cm^{-1}; no well-defined peaks could be observed mainly due to the highly disordered structure of the BCN films and the multiple bonding arrangements as revealed by XPS analysis below. In fact, several bond types involving boron, carbon, and nitrogen can appear in this wavenumber range, e.g., cubic BN phase at 1070 cm^{-1}, B−C stretching vibration from 1090 to 1250 cm^{-1} depending on the chemical environment,[30] and C−N (sp) and C=N (sp^2) bonds at 1272 and 1540 cm^{-1}, respectively. Overlapping of these individual bands and short range order of structural crystallinity prevent resolving these chemical states in the FTIR spectra.

In complement to the FTIR measurements, XPS analysis was carried out to study the atomic composition and chemical states. Fig. 2 presents high resolution XPS B1s, N1s, and C1s core level spectra of the BCN films after Ar ion sputter cleaning. By calculating the integrated areas of the corresponding peaks corrected for sensitivity, the atomic concentrations of boron, carbon, nitrogen, and oxygen (denoted [B], [C], [N], and [O], respectively) before sputter cleaning were 30.0, 24.3, 30.6, and 15.1 at. %, respectively. After Ar ion sputter cleaning, [C] and [O] decreased to 11.1 and 5.7 at. %, whereas the portions of [B] and [N] increased to 44.5 and 38.7 at. %, respectively. This indicates that the adventitious hydrocarbon and oxygen-based contaminants adsorbed on the surface were removed.

The broad and asymmetric peaks of B1s, N1s, and C1s imply the existence of multiple chemical environments in the BCN matrix. The B1s spectrum in Fig. 2(a) could be deconvoluted into three peaks located at 189.6, 191.0, and 192.2 eV. The dominant component centered at 191.0 eV is assigned to B−N bonds. The smaller shoulders peaking at 189.6 and 192.2 eV are attributed to B−C and B−O bonds, respectively.[31] In the N1s spectrum (Fig. 2(b)), the major component at 398.5 eV originates from N−B bonding,

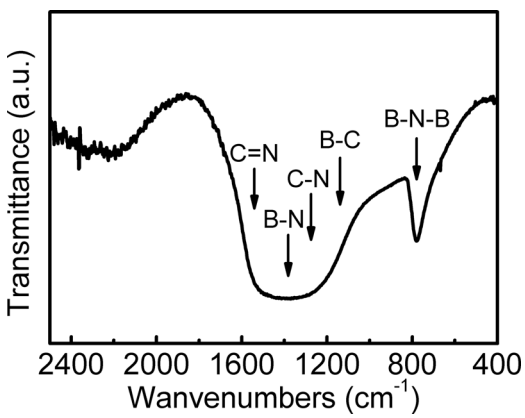

FIG. 1. Representative FTIR spectrum collected from a pristine BCN film.

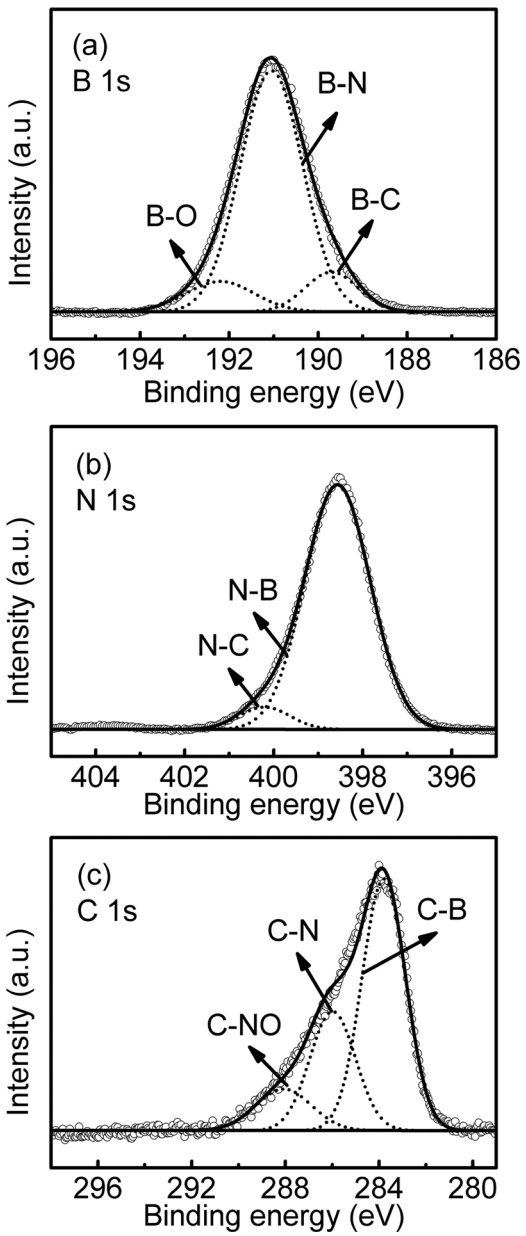

FIG. 2. High resolution XPS spectra obtained from a pristine BCN film: (a) B1s, (b) N1s, and (c) C1s core level spectra. The open circles are the raw data; the solid lines are backgrounds and fitted curves, while the dashed lines are deconvoluted peaks corresponding to different chemical states.

consistent with the corresponding chemical state in the B1s spectrum. The component located at 400.2 eV suggests the formation of sp^2 N−C bonds.[32,33]

Since the percentage of each chemical state is proportional to the integral area of the resulting deconvoluted peak, it is found that the abundance of B−N bonds is much higher than that of B−C bonds. Deconvolution of the C1s peak in Fig. 2(c) reveals the C−B bonding at 283.6 eV, the sp^2 C−N bonding at 286 eV, and the C−NO bonding at 288.1 eV. The presence of B−O and C−NO bonds is due to residual surface oxides which are more resistant to the sputter cleaning process than the physically adsorbed surface contaminants. Both the FTIR and XPS analyses imply that the ternary BCN films are amorphous and composed of B−N, C−N, and B−C bonds.

Hall measurements showed that the BCN films exhibit p-type conductivity and a carrier mobility of 1−5 $cm^2/V{\cdot}s$ at room temperature. In comparison, the carrier mobility of polycrystalline BCN films deposited by CVD at a substrate temperature of ∼850 °C was reported to be in the range of 0.37–30 $cm^2/V{\cdot}s$ depending on the film microstructure.[13,34] The low carrier mobility of the BCN films in this work is due to their amorphous nature and it needs to be further improved for their electronic applications.

The optical properties of the BCN films were studied by UV/Vis spectroscopy. A representative UV-Vis absorption spectrum of the BCN films deposited on fused silica substrates is shown in Fig. 3. The films exhibit a fairly broad absorption band ranging from the visible to the near-infrared region. The interference fringes observed at the absorption edge are due to the multiple reflections in films. In the inset of Fig. 3, $(\alpha h\nu)^{1/2}$ is plotted as a function of photon energy ($h\nu$), where α is the absorption coefficient. From this function, known as the Tauc's plot, the optical band gap of the BCNs films is determined by an extrapolation method. The tangent intersect with the abscissa points to an optical band gap of 1.0 eV.

Thus, the Hall measurements and UV-Vis absorption analysis indicate that the BCN films are p-type semiconductor with a band gap of 1.0 eV. BCN is a complex ternary composite with electronic and electrical properties strongly influenced by the composition and phase structure which are strongly related to the deposition method and the deposition conditions. Early studies on BCN films reported a band gap of ∼3.0 eV when the films were synthesized by CVD at temperatures higher than 300 °C.[11] Elsewhere,[14] it was shown that the optical band gap of the BCN deposited by sputtering decreased from 2.0 to 1.5 eV as the deposition temperature decreased from 550 to 250 °C. In the presented work, the substrate temperature is below 100 °C that appears to result in a relatively narrow band gap of 1.0 eV.

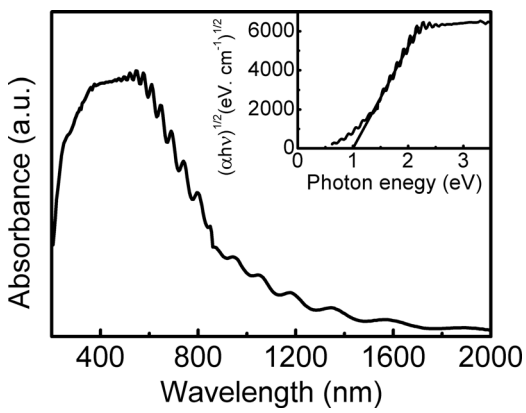

FIG. 3. UV-Vis absorption spectrum of a typical BCN film. The inset shows $(\alpha h\nu)^{1/2}$ plotted as a function of photon energy.

To facilitate p-n heterojunctions, ZnO NR arrays were grown on the BCN films by a low-temperature hydrothermal growth method. The cross-sectional SEM images in Fig. 4(a) show that the ZnO NRs are tightly bonded with the BCN films through a ZnO seeding layer, and no delamination between ZnO and BCN films was observed. ZnO NRs are grown uniformly over the BCN film with a typical length of 3 μm and a diameter of ∼200 nm in average; the density of the NRs is approximately $4.58 \times 10^8\,cm^{-2}$, and the NRs preferentially grow along the direction orthogonal to the substrate (i.e., along the *c*-axis of the ZnO lattice). Because of the inherent n-type conductivity of the ZnO NRs, p-n heterojunctions are formed between the BCN film and the ZnO NRs on the silicon substrate.

Al and Ag electrodes were employed to form ohmic contacts, as shown schematically in the insets of Fig. 4(b). The I-V characteristics of Ag/BCN and Al/ZnO ohmic junctions and BCN/ZnO-NRs heterojunctions are shown in Fig. 4(b). As the metal contacts to the films are ohmic in nature, a clear rectifying behavior of the junctions is revealed. The rectification ratio (the forward-to-reverse current ratio) as high as 1500 at relatively low bias voltages of ±5 V has been demonstrated. This rectification performance appears

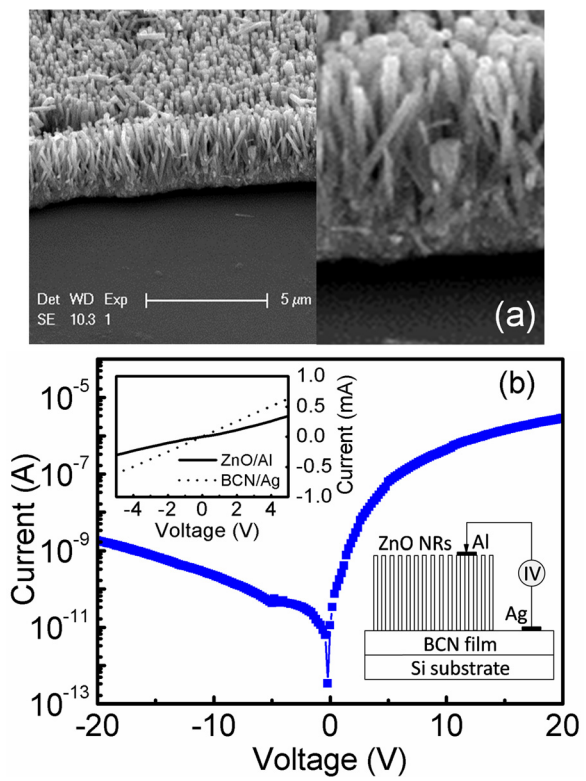

FIG. 4. (a) SEM image of ZnO NRs in a cross sectional view; (b) I-V characteristics of a BCN/ZnO NRs heterojunction. Inset shows the I-V characteristics of ZnO/Al and BCN/Ag ohmic contacts and the schematic configuration of the heterojunction.

significantly higher compared to our previous work on p-GaN/n-ZnO-NRs heterojunction LEDs with their rectification ratio of 320 at ±20 V.[35] In the case of ZnO/GaN heterostructures, one would expect a good lattice match as both the materials have hexagonal lattices, and their lattice parameters and band gap values are also very close. In contrast, in the case of BCN/ZnO heterostructures, such similarities are not expected. In fact, there are rather notable dissimilarities: ZnO is a wide gap semiconductor with a bandgap of 3.4 eV, while BCN is a narrow band gap semiconductor with a bandgap of ~1.0 eV. Thus, a large band bending would occur at the heterointerface in the valence band region.

The I-V curve of a p-n heterojunction could be simulated by Shockley equation (1) for an ideal diode

$$I = I_0\left[\exp\left(\frac{V}{nV_t} - 1\right)\right], \tag{1}$$

where I_0 is the saturation current, $V_t = kT/q$ is the thermal voltage, q is the electronic charge, n is the ideality factor, k is the Boltzmann constant, and T is the absolute temperature. The ideality factor could thus be calculated from the slope of the linear region in the ln (I)−V plot and expressed as

$$n = \frac{q}{kT}\frac{dV}{d(\ln I)}. \tag{2}$$

For $V < 0.5$ V, n was found to be around 2; for $V > 0.5$ V, it is much higher than 2. For an ideal p-n homojunction n is ~1, while in p-n homojunctions where the tunneling current mechanism is dominant, n is between 1 and 2. Considering the ideal diode model valid in the case of studied heterojunction diodes, dominance of tunneling current at low voltages appears to be valid in the first instance to explain the n of ~2. However, considering the band structure of the studied heterojunction, the inter-band direct tunneling appears unlikely at small forward bias voltages. In such case, impurity assisted tunneling or band to impurity cascade processes may contribute to the tunneling current.

There are a number of defects anticipated in the studied structure: (i) a large amount of defects in the as-deposited amorphous BCN films; (ii) electronic defects in the ZnO synthesized by low-temperature solution based process;[36] (iii) interface defects induced by the significant mismatch of the ZnO and BCN lattices.[37] Some of these defects can be optically as well as electrically active and influence the electrical transport.[38] Thus, a cascade of tunneling is possible in the studied heterostructures. At high bias voltages, a large deviation of n (>2) is noted. Very large values of n ($2 < n < 8$) have been reported for diodes based on AlGaN/GaN p-n heterojunctions and GaN LEDs[39,40] operating at high bias voltages.

Additional rectifying effects due to metal/semiconductor interfaces at high biases have been shown to contribute to the resulting rectification and the high value of n. Similar mechanism in the studied heterojunction is not unlikely. The demonstration of BCN based heterojunctions presented here shows their feasibility of application in electronic devices. However, further studies are necessary to better understand the electronic properties of BCN films and the transport mechanism behind the observed ideality factors.

In summary, BCN films were deposited by RF magnetron sputtering from a B_4C target using a N_2/Ar gas mixture. The atomic contents of boron, carbon, nitride, and oxygen were evaluated to be 44.5, 11.1, 38.7, and 5.7 at. %, respectively. The BCN films are composed of B−N, C−N, and B−C bonds in sp^2 and sp^3 configurations. The as-deposited BCN films show p-type conductivity with an optical band gap of 1.0 eV. ZnO NR arrays with n-type conductivity were grown on the BCN films to form p-n heterojunctions. The I-V characterization of the BCN/ZnO-NRs junctions shows a rectification behavior with a rectification ratio of 1500 at the bias voltages of ±5 V. The unique combination of optical and electronic properties of the BCN films with tunable optical band gap and the interesting device characteristics of the BCN/ZnO heterojunction diodes imply that the emerging ternary BCN materials are viable semiconductors for the fabrication of future electronic devices.

This work was supported by the Research Grants Council of the Hong Kong Special Administrative Region (Project No. CityU 104911), the National Science Foundation of China (NSFC Grant Nos. 61176007 and 51372213), and the Natural Sciences and Engineering Research Council (NSERC) of Canada.

[1]L. Filipozzi, A. Derre, J. Conard, L. Piraux, and A. Marchand, Carbon **33**(12), 1747 (1995).
[2]V. L. Solozhenko, D. Andrault, G. Fiquet, M. Mezouar, and D. C. Rubie, Appl. Phys. Lett. **78**(10), 1385 (2001).
[3]M. O. Watanabe, S. Itoh, K. Mizushima, and T. Sasaki, Appl. Phys. Lett. **68**(21), 2962 (1996).
[4]M. Kawaguchi, T. Kawashima, and T. Nakajima, Chem. Mater. **8**(6), 1197 (1996).
[5]H. Sota, C. Kimura, H. Aoki, and T. Sugino, Diam. Relat. Mater. **19**(12), 1441 (2010).
[6]Q. Yang, C. B. Wang, S. Zhang, D. M. Zhang, Q. Shen, and L. M. Zhang, Surf. Coat. Technol. **204**(11), 1863 (2010).
[7]H. Aoki, T. Masuzumi, M. Hara, D. Watanabe, C. Kimura, and T. Sugino, Thin Solid Films **518**(8), 2102 (2010).
[8]S. Ulrich, H. Ehrhardt, T. Theel, J. Schwan, S. Westermeyr, M. Scheib, P. Becker, H. Oechsner, G. Dollinger, and A. Bergmaier, Diam. Relat. Mater. **7**(6), 839 (1998).
[9]A. Lousa, J. Esteve, S. Muhl, and E. Martínez, Diam. Relat. Mater. **9**(3–6), 502 (2000).
[10]R. Gago, I. Jimenez, J. M. Albella, and L. J. Terminello, Appl. Phys. Lett. **78**(22), 3430 (2001).
[11]T. Yuki, S. Umeda, and T. Sugino, Diam. Relat. Mater. **13**(4–8), 1130 (2004).
[12]M. O. Watanabe, S. Itoh, K. Mizushima, and T. Sasaki, J. Appl. Phys. **78**(4), 2880 (1995).
[13]M. O. Watanabe, S. Itoh, T. Sasaki, and K. Mizushima, Phys. Rev. Lett. **77**(1), 187 (1996).
[14]M. K. Lei, Q. Li, Z. F. Zhou, I. Bello, C. S. Lee, and S. T. Lee, Thin Solid Films **389**(1–2), 194 (2001).
[15]H. Ahn, L. Alberts, J. Wöhle, and K. T. Rie, Surf. Coat. Technol. **142–144**(0), 894 (2001).
[16]M. Watanabe, K. Mizushima, S. Itoh, and M. Mashita, U.S. patent 5,895,938 A (April 20, 1999).
[17]B. W. Robertson, S. Adenwalla, A. Harken, P. Welsch, J. I. Brand, P. A. Dowben, and J. P. Claassen, Appl. Phys. Lett. **80**(19), 3644 (2002).
[18]S. D. Hwang, K. Yang, P. A. Dowben, A. A. Ahmad, N. J. Ianno, J. Z. Li, J. Y. Lin, H. X. Jiang, and D. N. McIlroy, Appl. Phys. Lett. **70**(8), 1028 (1997).
[19]S. Adenwalla, P. Welsch, A. Harken, J. I. Brand, A. Sezer, and B. W. Robertson, Appl. Phys. Lett. **79**(26), 4357 (2001).
[20]E. Day, M. J. Diaz, and S. Adenwalla, J. Phys. D: Appl. Phys. **39**(14), 2920 (2006).
[21]A. N. Caruso, R. B. Billa, S. Balaz, J. I. Brand, and P. A. Dowben, J. Phys.: Condens. Matter **16**(10), L139 (2004).

[22]G. D. Yuan, W. J. Zhang, J. S. Jie, X. Fan, J. X. Tang, I. Shafiq, Z. Z. Ye, C. S. Lee, and S. T. Lee, Adv. Mater. **20**(1), 168 (2008).
[23]C. Levy-Clement, R. Tena-Zaera, M. A. Ryan, A. Katty, and G. Hodes, Adv. Mater. **17**(12), 1512 (2005).
[24]S. K. Jha, C. Luan, C. H. To, O. Kutsay, J. Kovac, J. A. Zapien, I. Bello, and S. T. Lee, Appl. Phys. Lett. **101**(21), 211116 (2012).
[25]M. Law, L. E. Greene, J. C. Johnson, R. Saykally, and P. D. Yang, Nat. Mater. **4**(6), 455 (2005).
[26]C. P. Liu, Z. H. Chen, H. E. Wang, S. K. Jha, W. J. Zhang, I. Bello, and J. A. Zapien, Appl. Phys. Lett. **100**(24), 243102 (2012).
[27]S. K. Jha, O. Kutsay, I. Bello, and S. T. Lee, J. Lumin. **133**(0), 222 (2013).
[28]L. E. Greene, B. D. Yuhas, M. Law, D. Zitoun, and P. Yang, Inorg. Chem. **45**(19), 7535 (2006).
[29]W. J. Zhang, Y. M. Chong, I. Bello, and S. T. Lee, J. Phys. D: Appl. Phys. **40**(20), 6159 (2007).
[30]X. M. Yang, X. M. Wu, L. J. Zhuge, and F. Zhou, Appl. Surf. Sci. **255**(7), 4279 (2009).
[31]H. Ling, J. D. Wu, J. Sun, W. Shi, Z. F. Ying, and F. M. Li, Diam. Relat. Mater. **11**(9), 1623 (2002).
[32]E. Ech-chamikh, A. Essafti, Y. Ijdiyaou, and M. Azizan, Sol. Energy Mater. Sol. Cells **90**(10), 1420 (2006).
[33]D. Marton, K. J. Boyd, A. H. Al-Bayati, S. S. Todorov, and J. W. Rabalais, Phys. Rev. Lett. **73**(1), 118 (1994).
[34]M. O. Watanabe, T. Sasaki, S. Itoh, and K. Mizushima, Thin Solid Films **281–282**(0), 334 (1996).
[35]S. Jha, J. C. Qian, O. Kutsay, J. Kovac, C. Y. Luan, J. A. Zapien, W. J. Zhang, S. T. Lee, and I. Bello, Nanotechnology **22**(24), 245202 (2011).
[36]L. Schmidt-Mende and J. L. MacManus-Driscoll, Mater. Today **10**(5), 40 (2007).
[37]Y. Gong, T. Andelman, G. Neumark, S. O'Brien, and I. Kuskovsky, Nanoscale Res. Lett. **2**(6), 297 (2007).
[38]N. Bano, I. Hussain, O. Nur, M. Willander, and P. Klason, J. Nanomater. **2010**, 1 (2010).
[39]H. C. Casey, J. Muth, S. Krishnankutty, and J. M. Zavada, Appl. Phys. Lett. **68**(20), 2867 (1996).
[40]J. M. Shah, Y. L. Li, T. Gessmann, and E. F. Schubert, J. Appl. Phys. **94**(4), 2627 (2003).